Electronic Supplementary Material (ESI) for Dalton Transactions.

Exploring the Phototoxicity of GSH resistant 2-(5, 6-dichloro-1H-benzo[d]imidazol-2-yl)quinoline-based Ir(III)-PTA complex in MDA-MB-231 Cancer Cell

Utpal Das, Priyankar Paira*

Department of Chemistry, School of advanced sciences, Vellore Institute of Technology Vellore-632014, Tamilnadu, India, E-mail: priyankar.paira@vit.ac.in

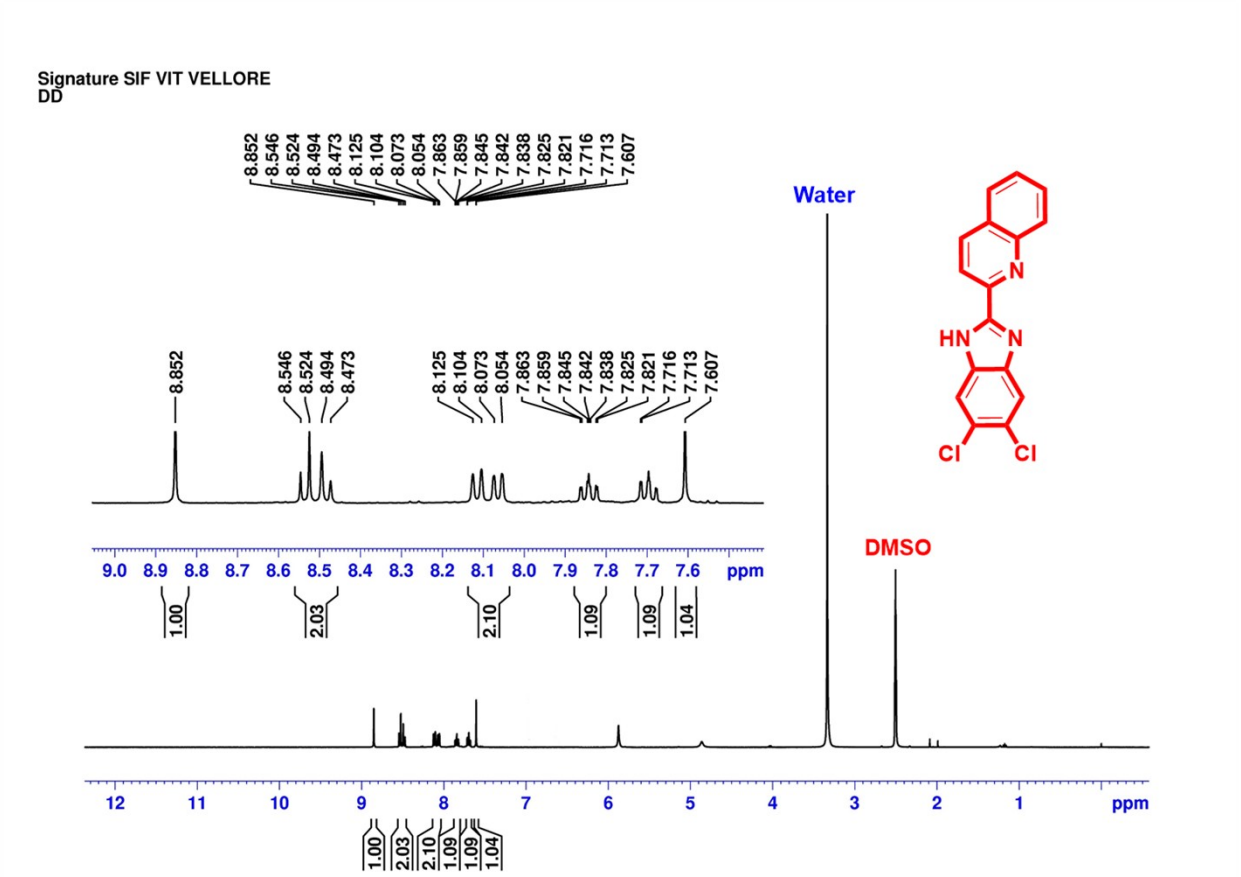

Fig. S1: ^{1}H NMR of ligand DD

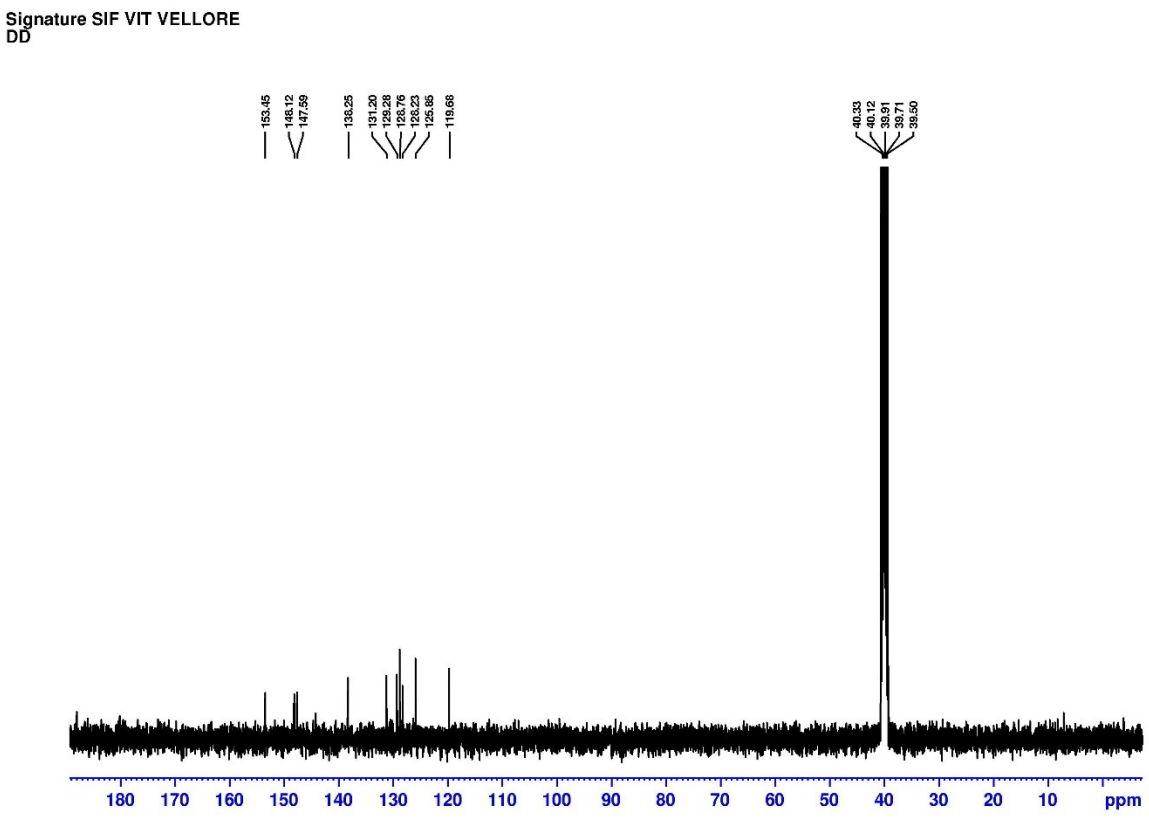

Fig. S2: ^{13}C NMR of ligand DD

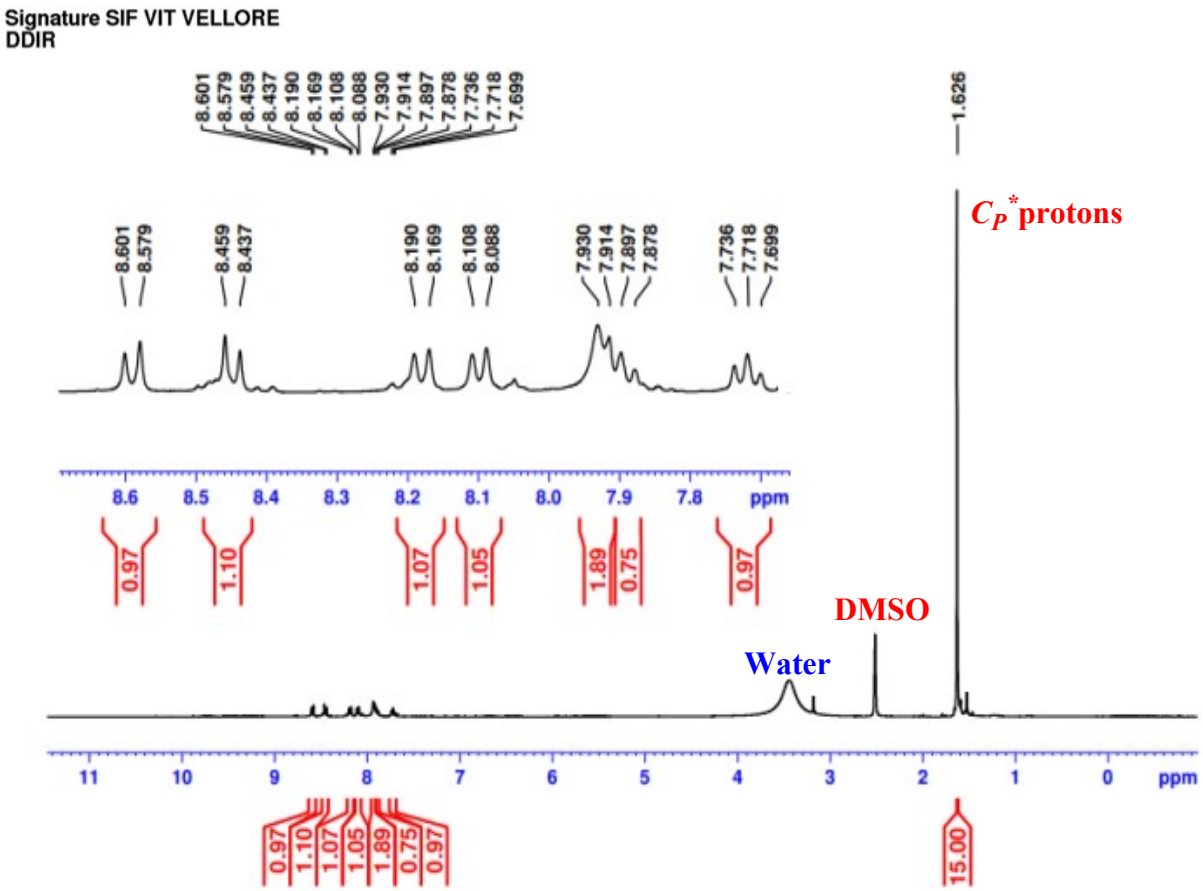

Fig. S3: ^{1}H NMR of complex DDIR

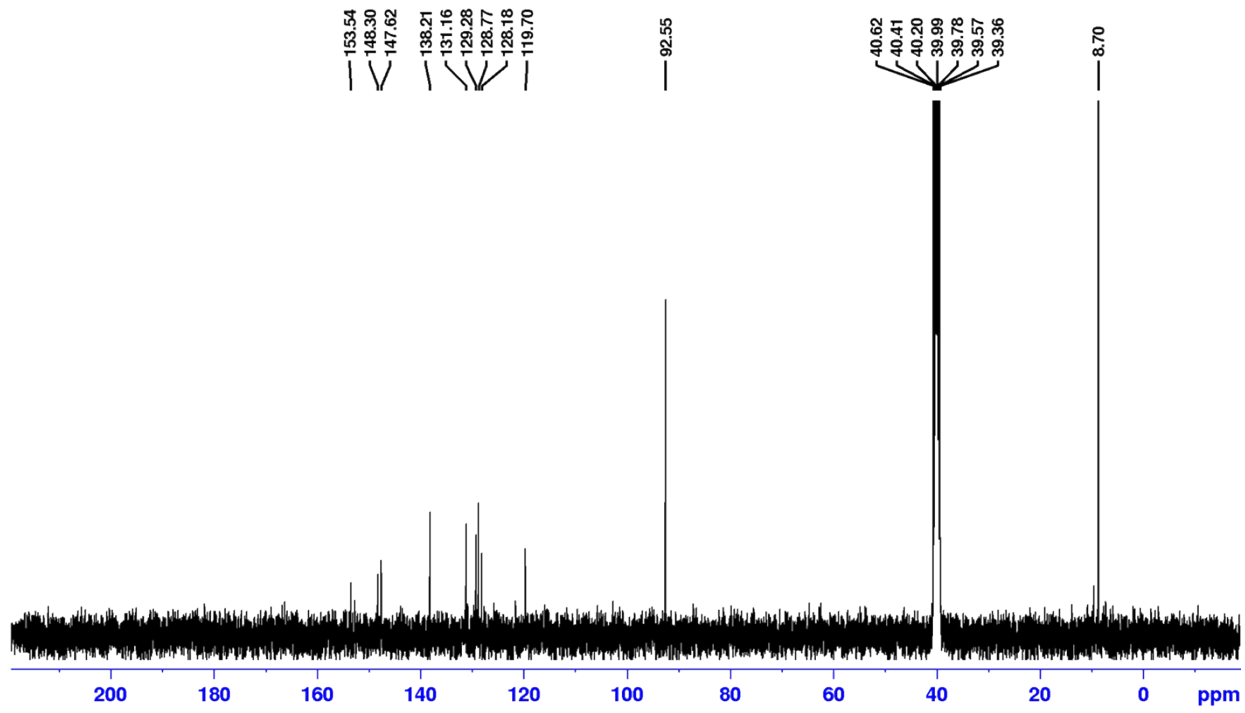

Fig. S4: ^{13}C NMR of complex DDIR

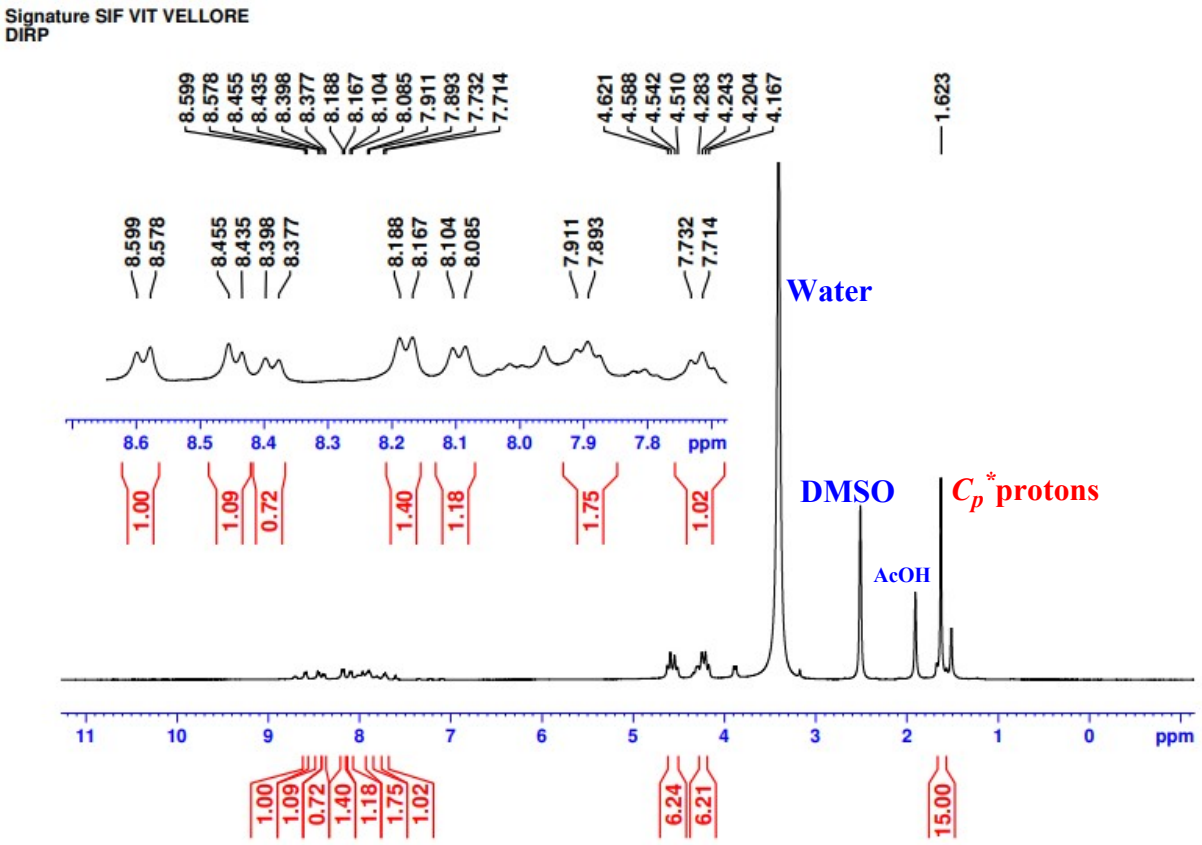

Fig. S5: ^{1}H NMR of complex DDIRP

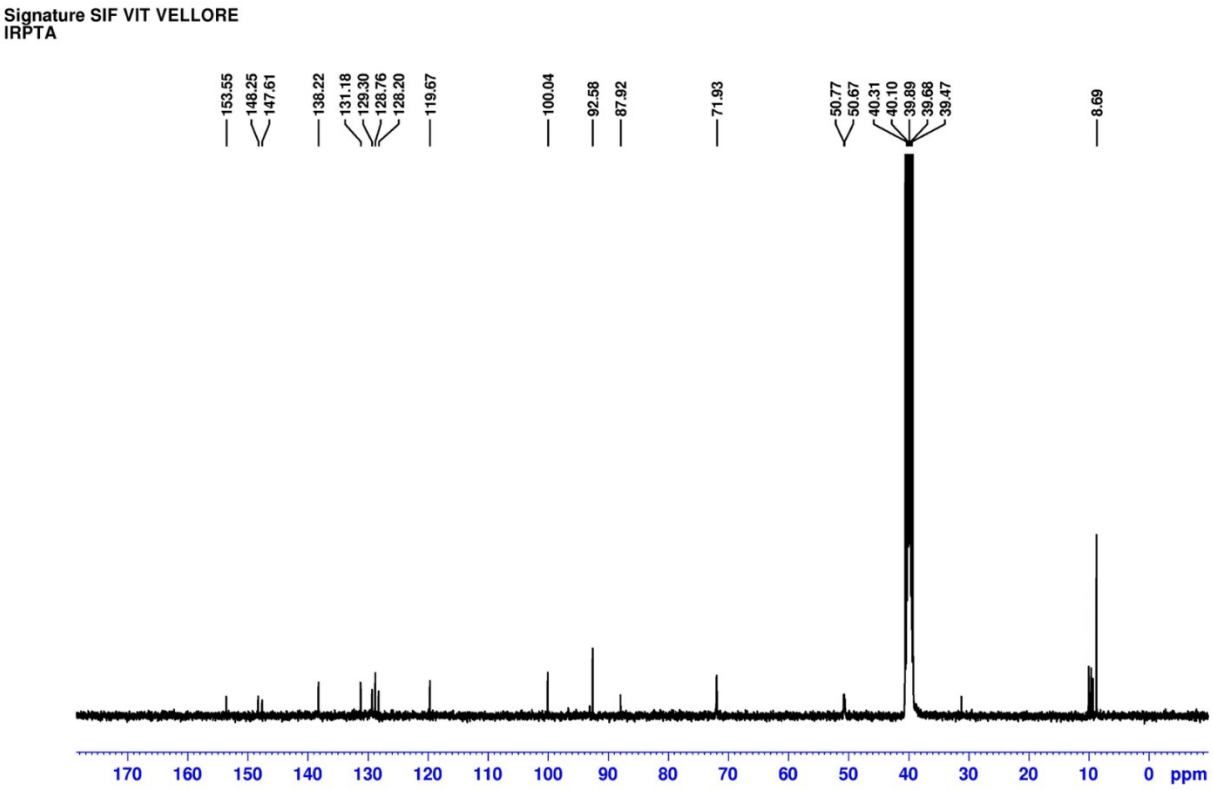

Fig. S6: ^{13}C NMR of complex DDIRP

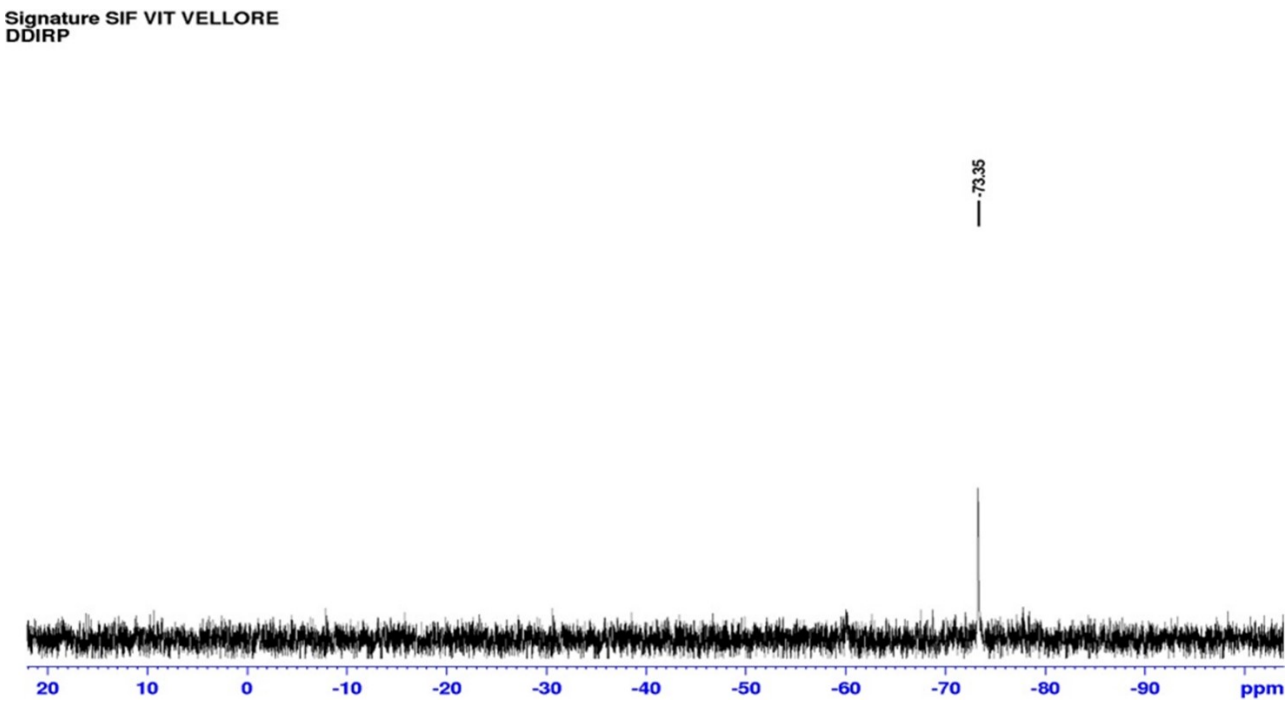

Fig. S7: ^{31}P NMR of complex DDIRP

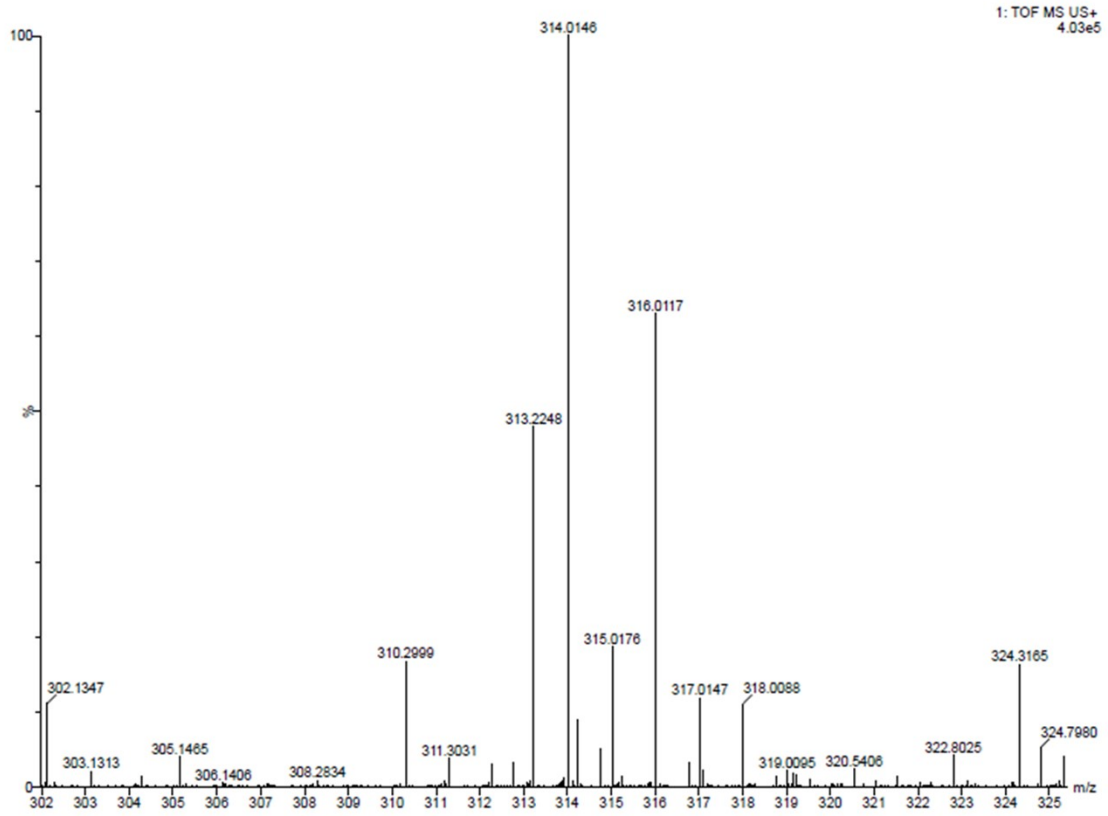

Fig. S8: ESI-HRMS spectra of DD in MeOH: $[DD+H]^+$ m/z 314.0146 (Calc: 314.0251).

(a)

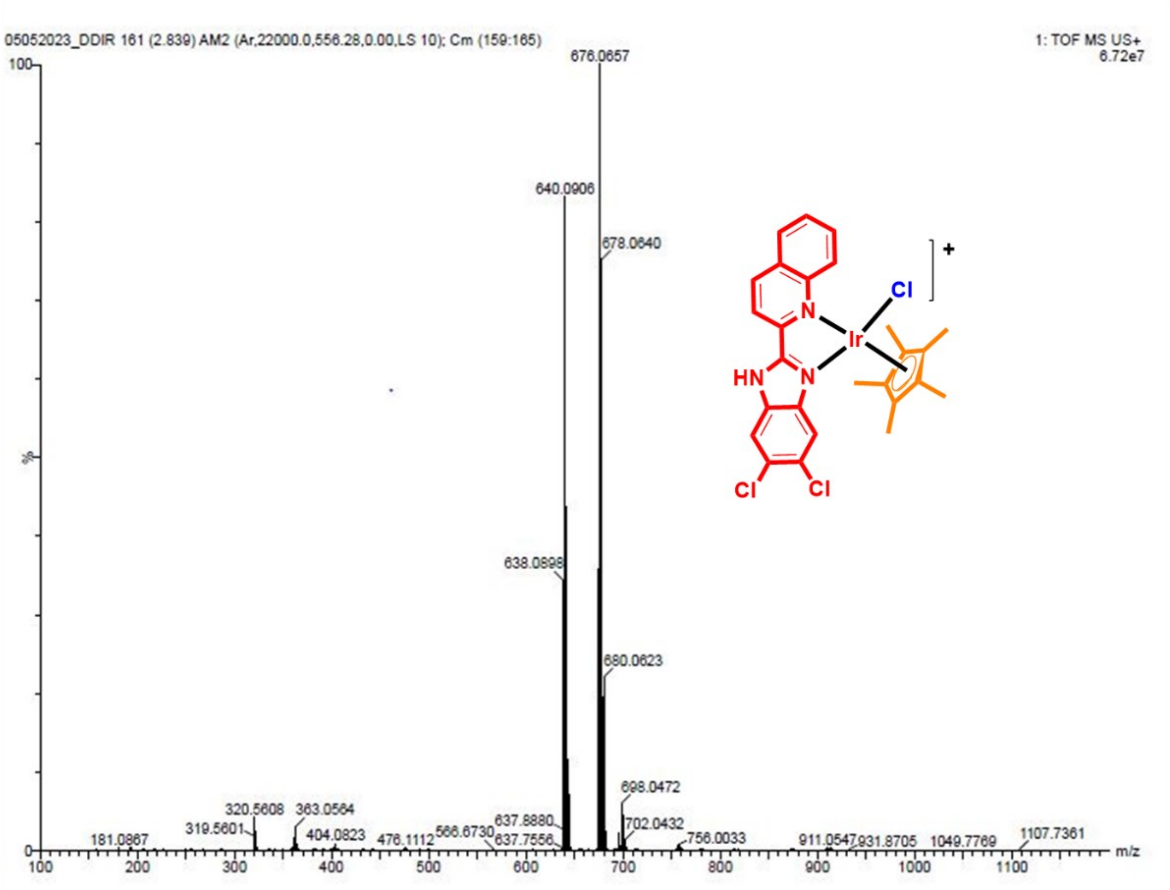
05052023_DDIR 161 (2.839) AM2 (Ar,22000.0,556.28,0.00,LS 10); Cm (159:165)
1: TOF MS US+
6.72e7
100
%
0
676.0657
640.0906
678.0640
638.0898
680.0623
698.0472
702.0432
320.5608
363.0564
319.5601
404.0823
637.8880
637.7556
566.6730
476.1112
181.0867
756.0033
911.0547
931.8705
1049.7769
1107.7361
100
200
300
400
500
600
700
800
900
1000
1100
m/z
Cl
Ir
N
HN
N
Cl
Cl
+

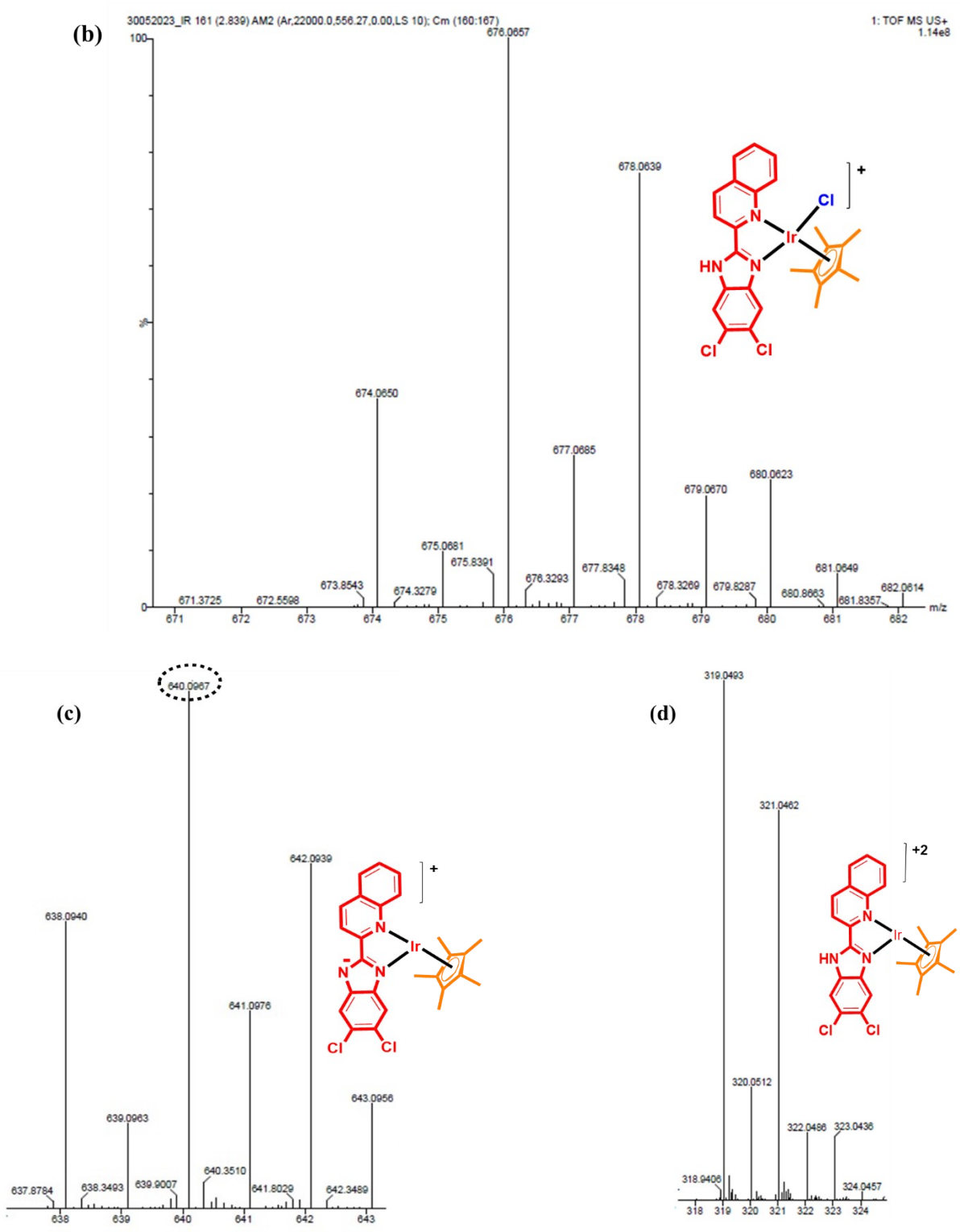

Fig. S9: ESI-HRMS spectra of DDIR in MeOH: (a) overall spectrum (b) Expand spectrum, m/z 676.0657 (Calc: 676.0665). (c) isotopic distribution of

hydrolyzed complex DDIR with m/z 640.0967 (Calc: 640.0898), (d) isotopic distribution of hydrolyzed complex DDIR with m/z 320.0512 (Calc: 320.5488).

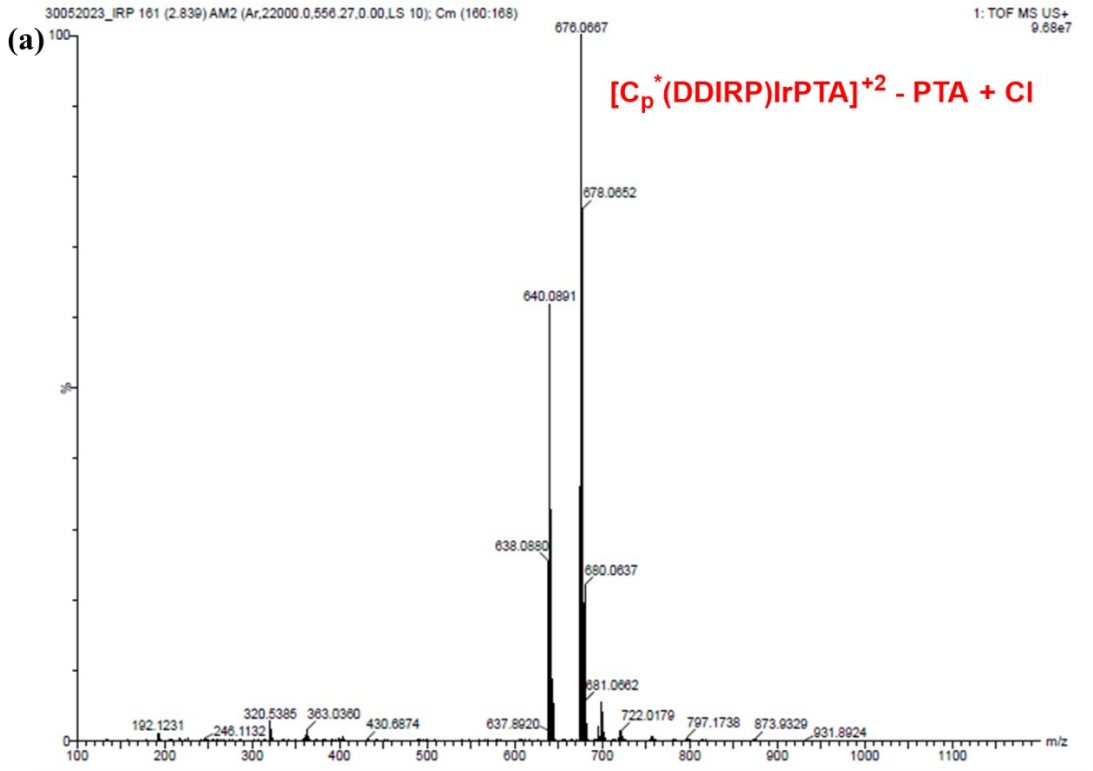

(b)

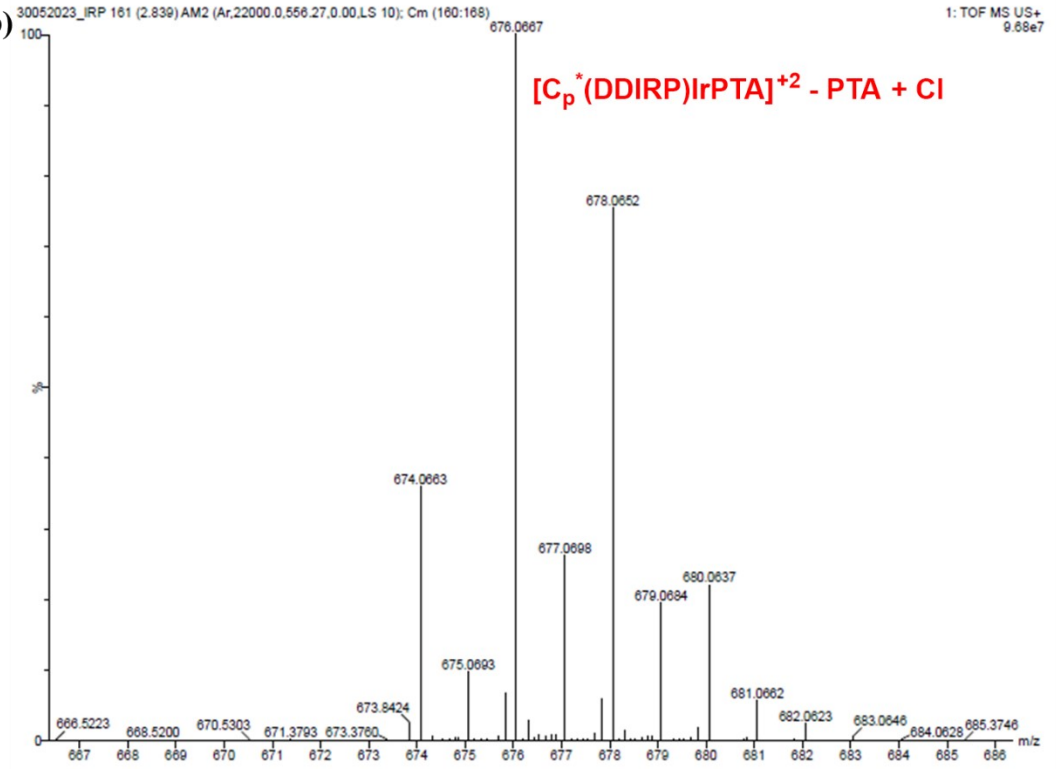
30052023_IRP 161 (2.839) AM2 (Ar,22000.0,556.27,0.00,LS 10); Cm (160:168)
1: TOF MS US+
9.68e7
[Cp*(DDIRP)IrPTA]+2 - PTA + Cl
676.0667
678.0652
674.0663
677.0698
680.0637
679.0684
675.0693
681.0662
673.8424
682.0623
683.0646
666.5223
668.5200
670.5303
671.3793
673.3760
684.0628
685.3746
m/z

(c)

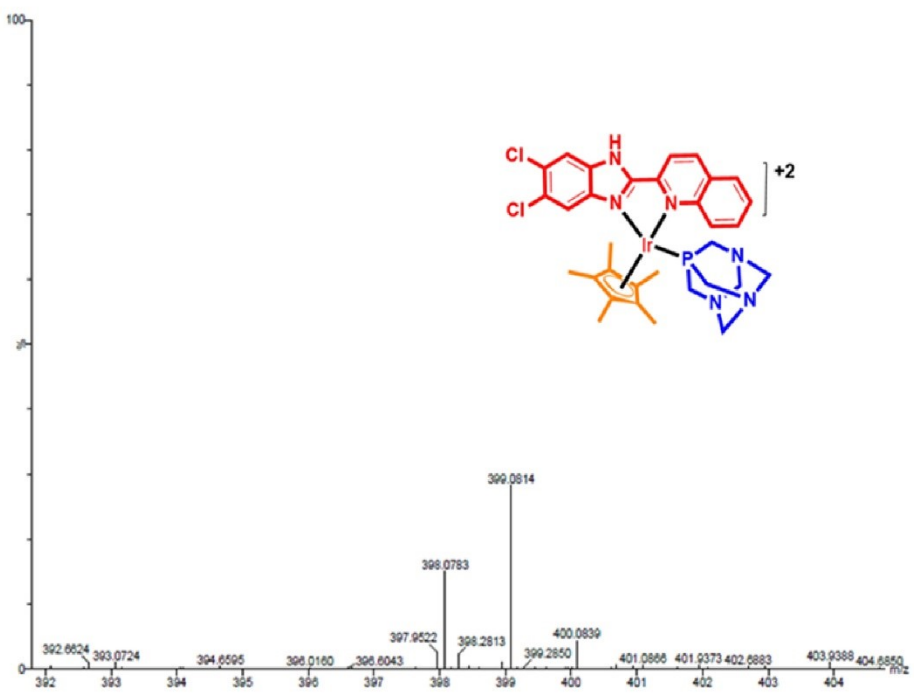
399.0814
398.0783
397.9522
398.2813
400.0839
392.6624
393.0724
394.6595
396.0160
396.6043
399.2850
401.0866
401.9373
402.6883
403.9388
404.6850
m/z

Cl
Cl
H
N
N
N
Ir
P
N
N
N
+2

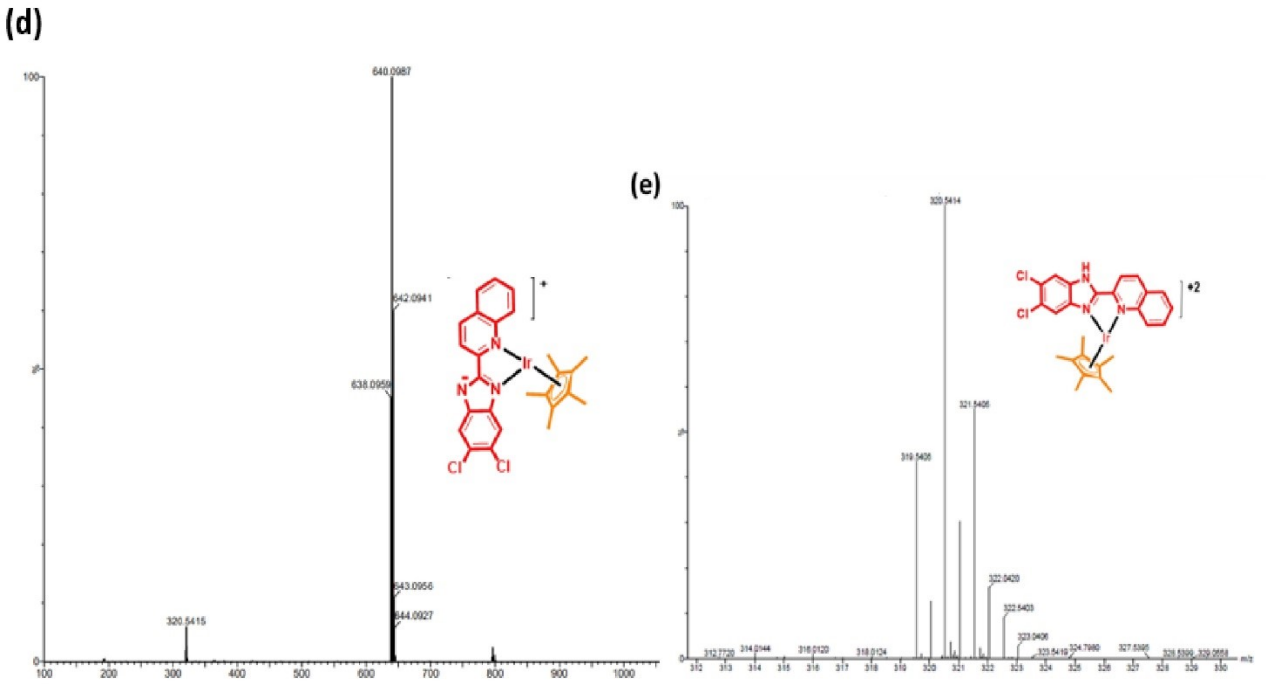

Fig. S10: ESI-HRMS spectra of DDIRP in MeOH: (a) overall spectrum (b) Expand spectrum, m/z 676.0667 (Calc: 676.0665), (c) isotopic distribution of complex DDIRP with m/z 399.0814 (Calc: 399.0872), (d) isotopic distribution of hydrolyzed complex DDIRP with m/z 640.0987 (Calc: 640.0898), (e) isotopic distribution of hydrolyzed complex DDIRP with m/z 320.5414 (Calc: 320.5488).

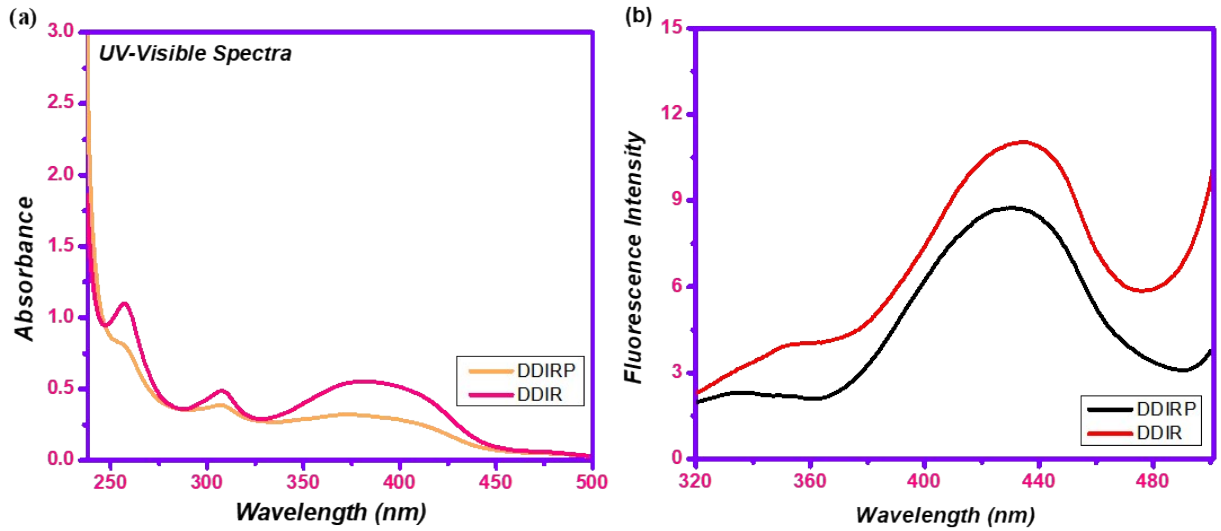

Fig. S11: (a) UV-Vis spectra of complexes DDIR and DDIRP in 5% DMSO-Water medium, (b) Emission spectra of complexes DDIR and DDIRP at 258 nm.

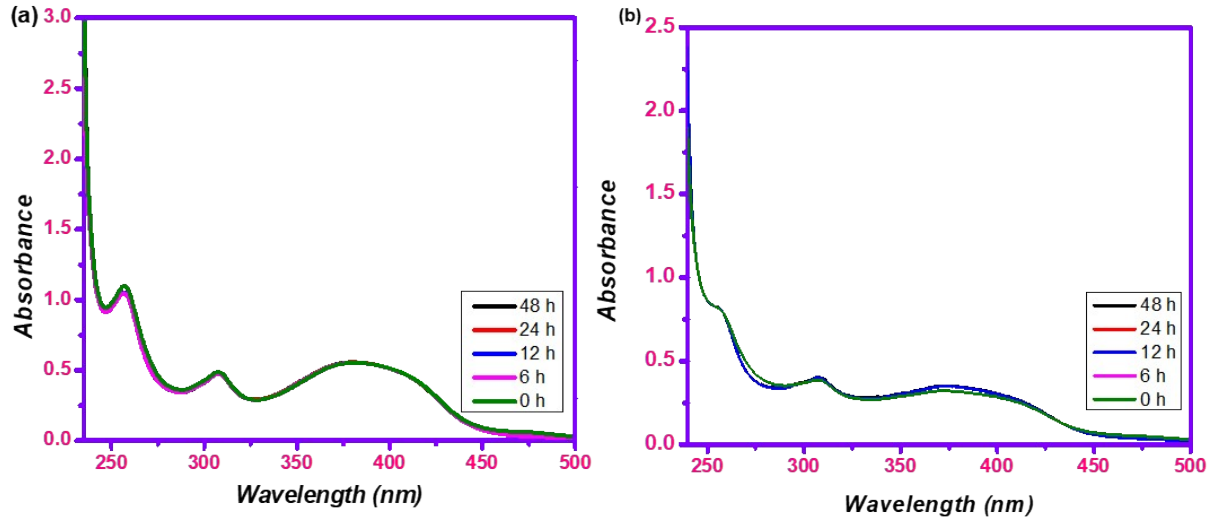

Fig. S12: Stability of complexes DDIR (a) and DDIRP (b) in 5% DMSO-Water medium.

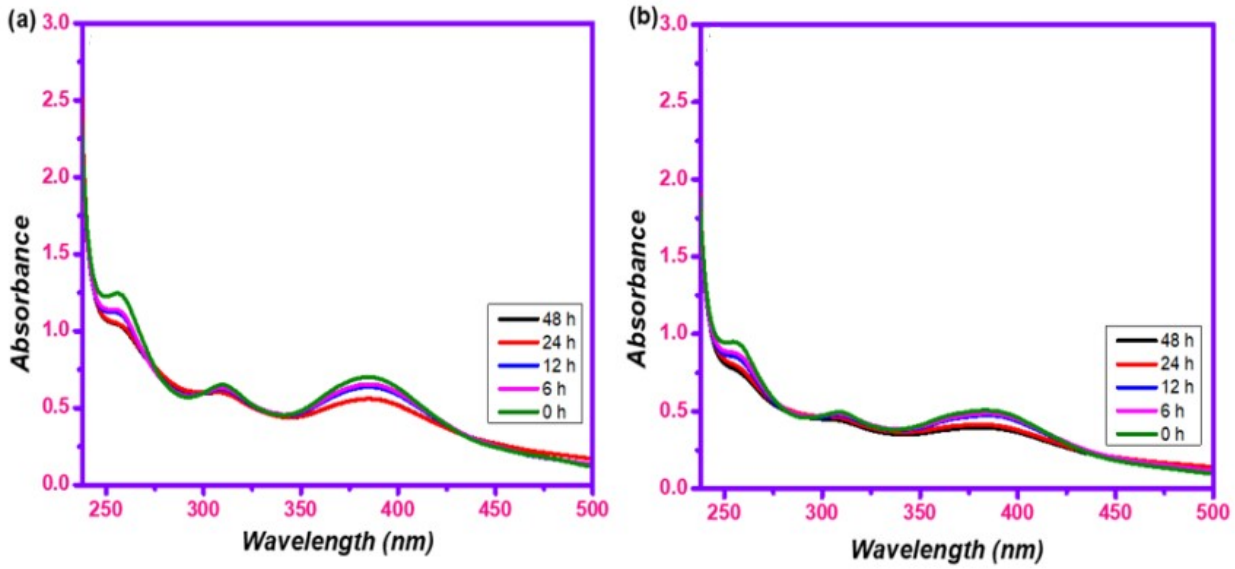

Fig. S13: Stability of complexes DDIR (a) and DDIRP (b) with 5% DMSO-PBS buffer in presence of 4 mM NaCl.

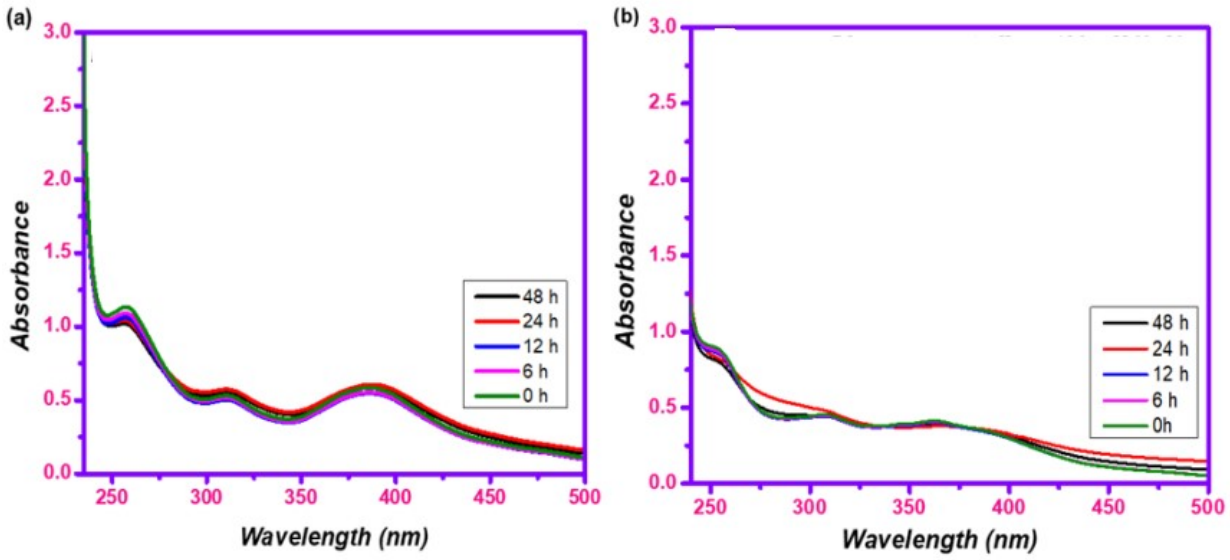

Fig. S14: Stability of complexes DDIR (a) and DDIRP (b) with 5% DMSO-PBS buffer in the presence of 120 mM NaCl.

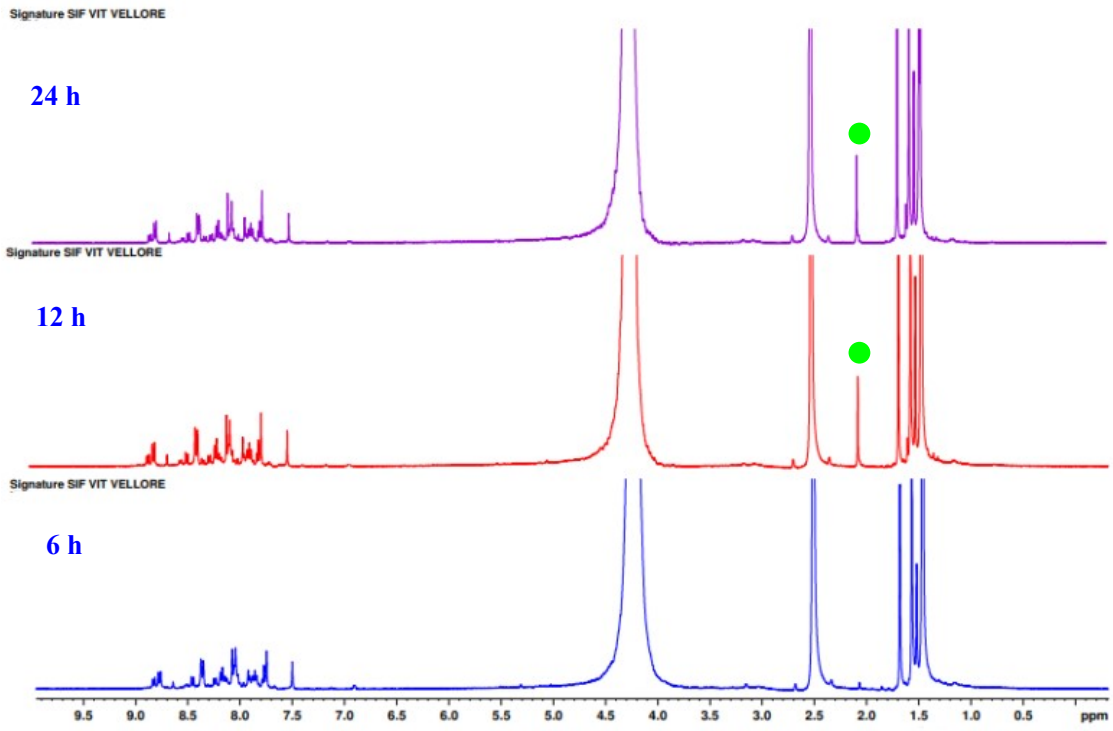

Fig. S15 Stability study of DDIR by ^{1}H NMR spectrum in DMSO-d_6/D_2O (4:2). "Green circle" stands for new peaks.

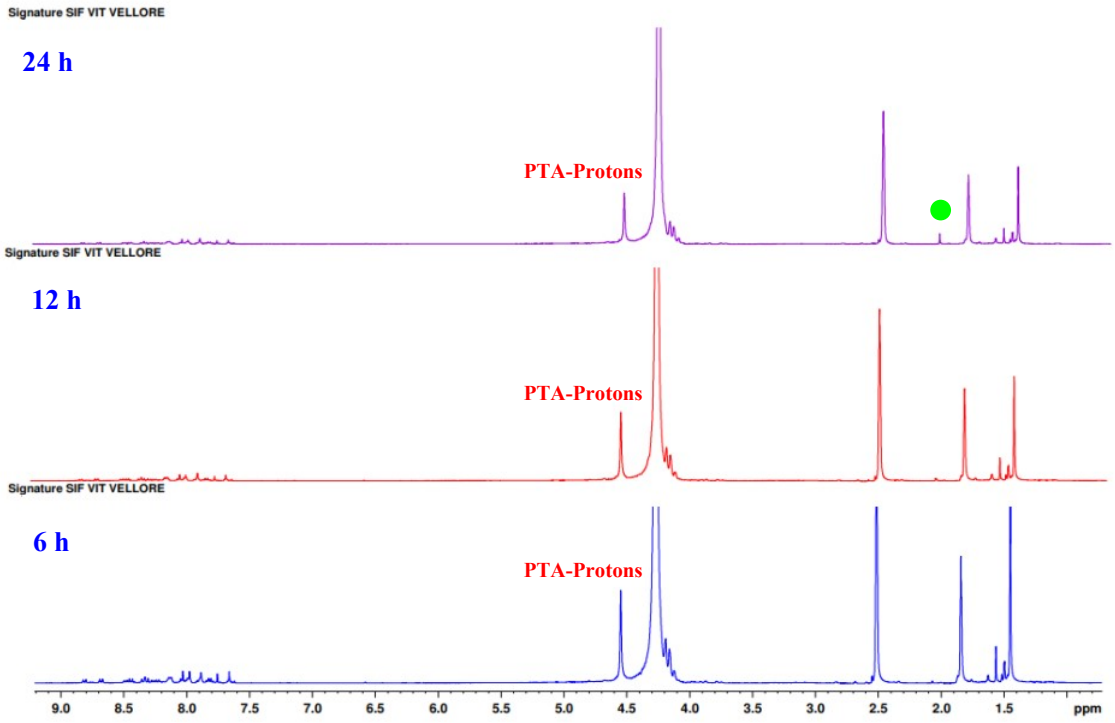

Fig. S16 Stability study of DDIRP by ^{1}H NMR spectrum in DMSO-d_6/D_2O (4:2). "Green circle" stands for new peaks.

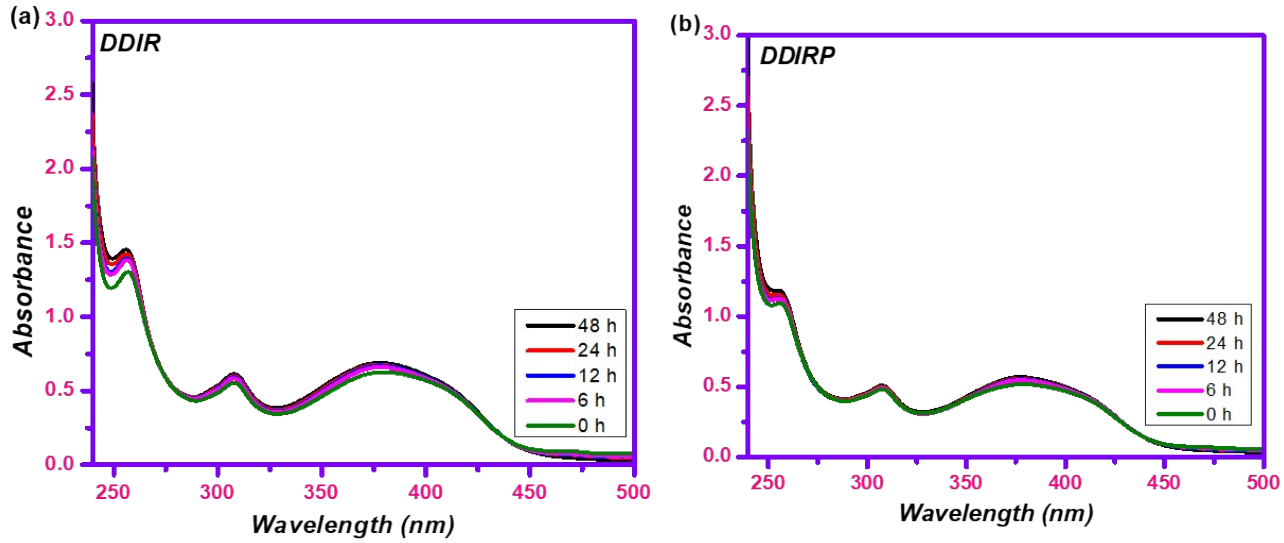

Fig. S17: Stability of complexes DDIR (a) and DDIRP (b) in 1 mM GSH solution in presence of 4 mM NaCl.

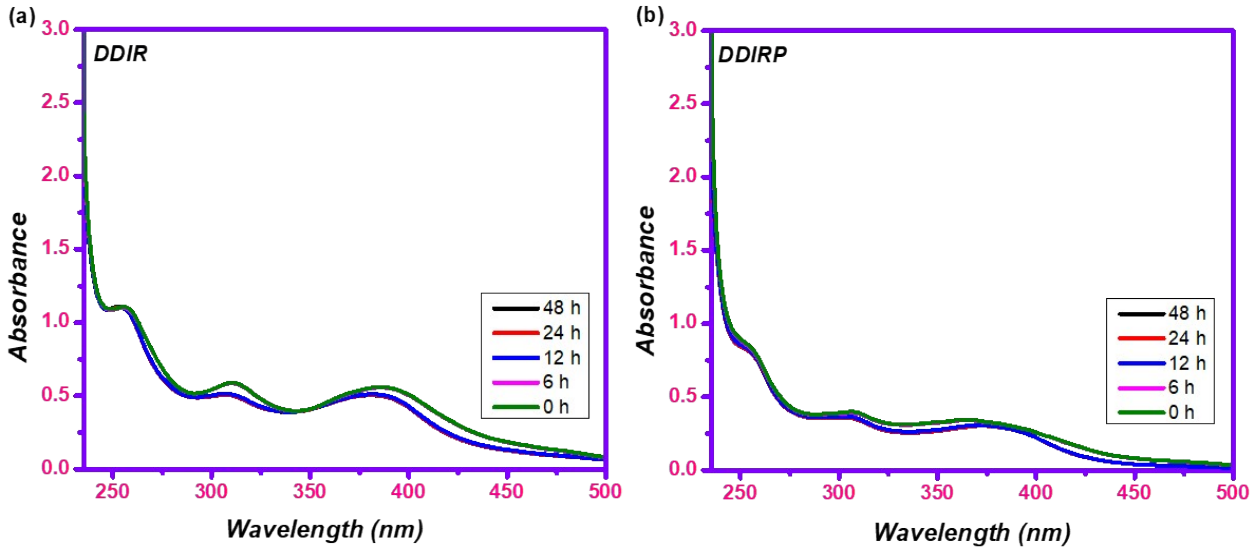

Fig. S18: Stability of complexes DDIR (a) and DDIRP (b) in 1 mM GSH solution in the presence of 120 mM NaCl.

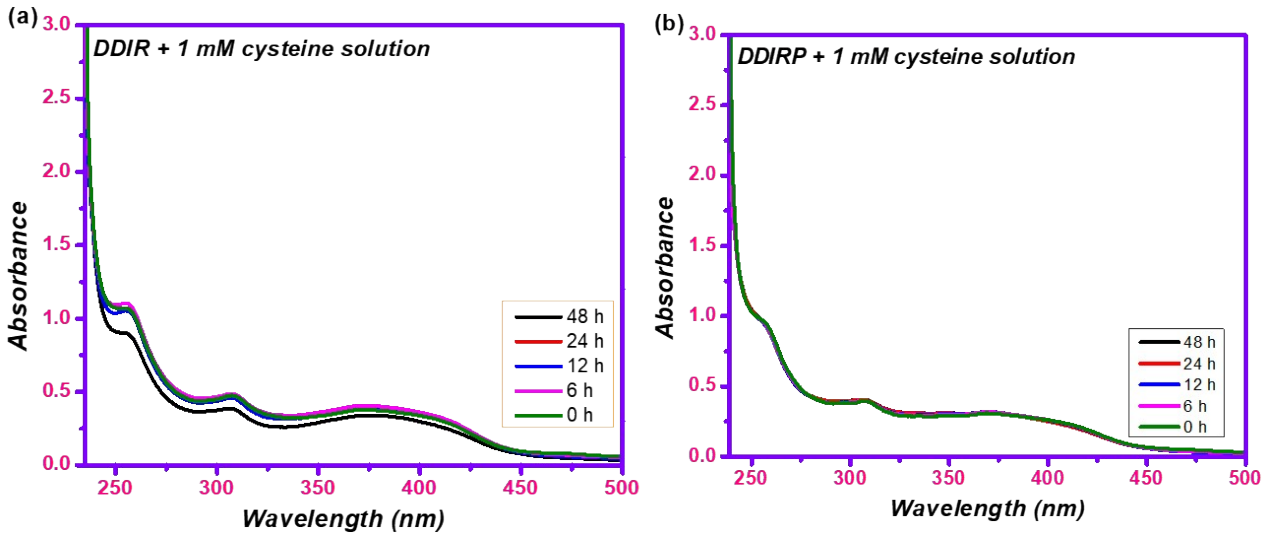

Fig. S19: Stability of complexes DDIR (a) and DDIRP (b) in 1 mM Cysteine solution.

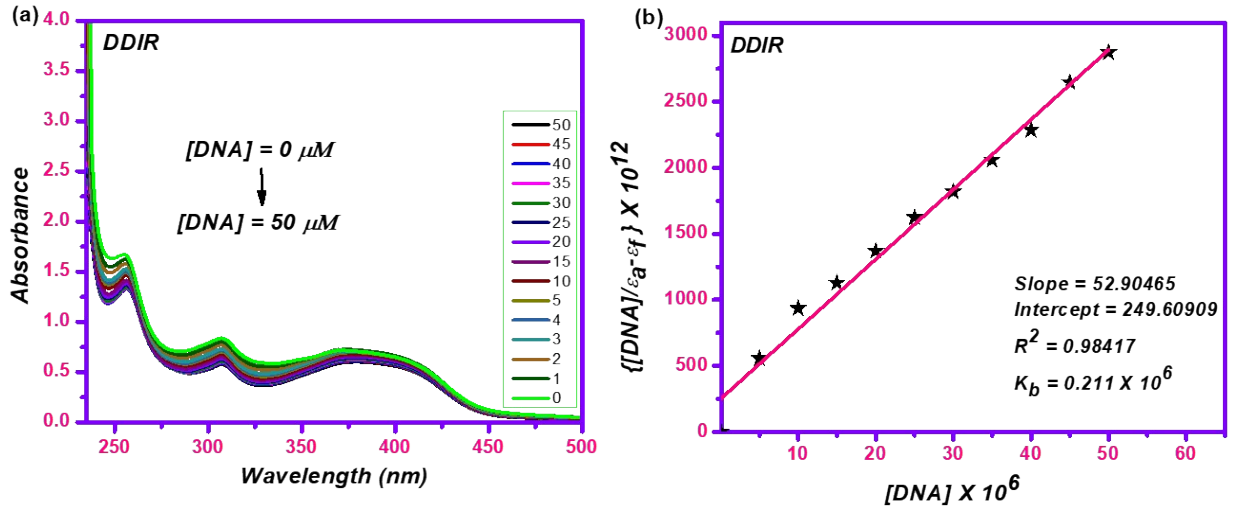

Fig. S20: DNA binding plots of complex DDIR (a), [DNA]/ (ε_a-ε_f) vs [DNA] linear plot of complex DDIR (b).

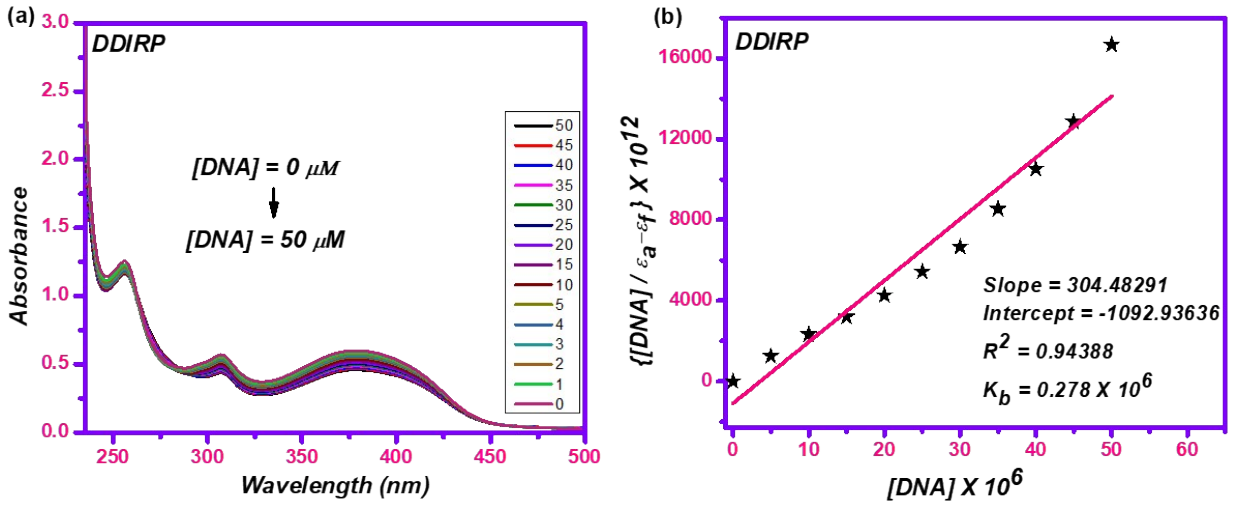

Fig. S21: DNA binding plots of complex DDIRP (a), [DNA]/ (ε_a-ε_f) vs [DNA] linear plot of complex DDIRP (b).

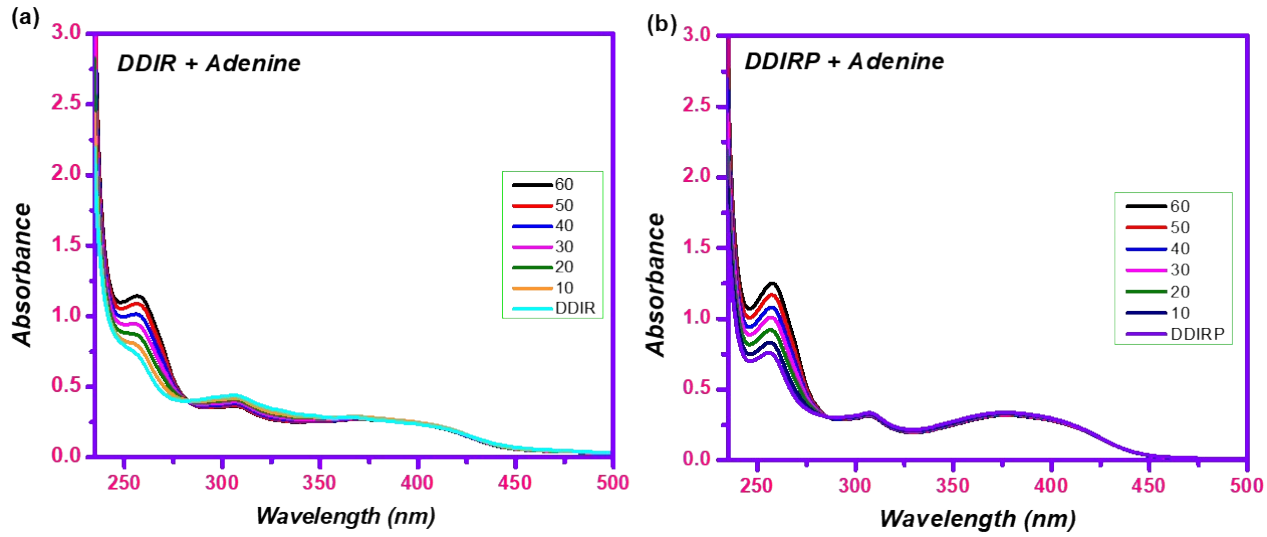

Fig. S22: Concentration-dependent binding study of DDIR (a) and DDIRP (b) complexes with 1 mM Adenine solution.

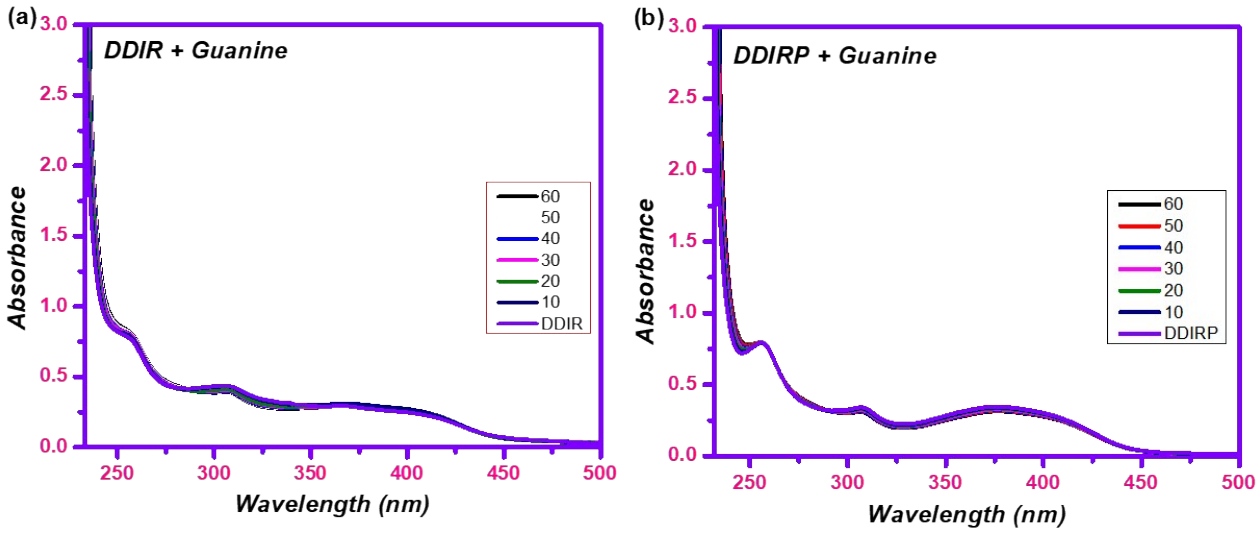

Fig. S23: Concentration-dependent binding study of DDIR (a) and DDIRP (b) complexes with 1 mM Guanine solution.

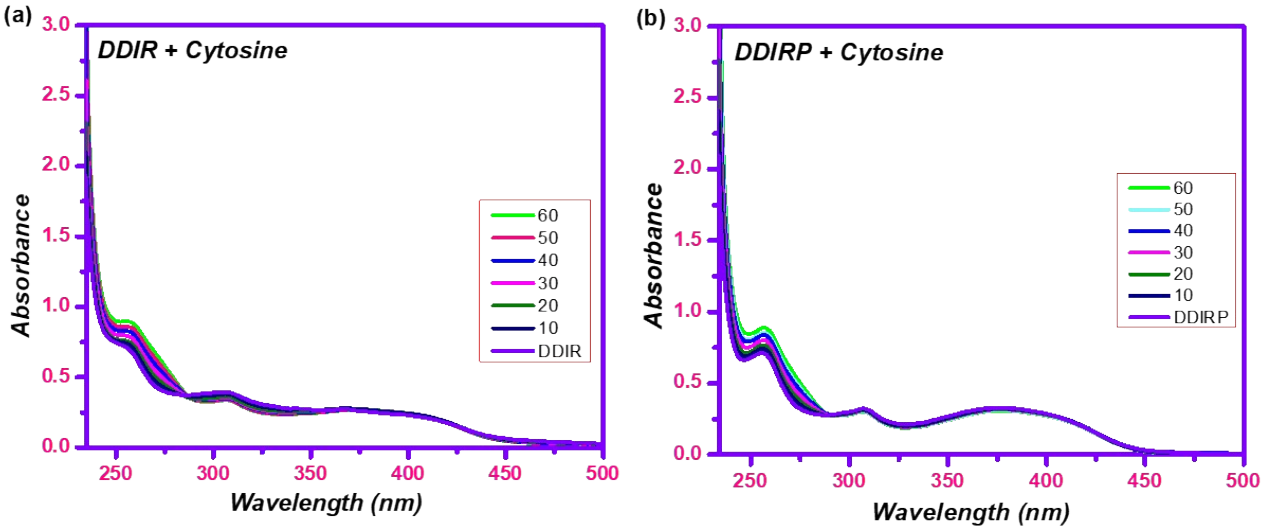

Fig. S24: Concentration-dependent binding study of DDIR (a) and DDIRP (b) complexes with 1 mM Cytosine solution.

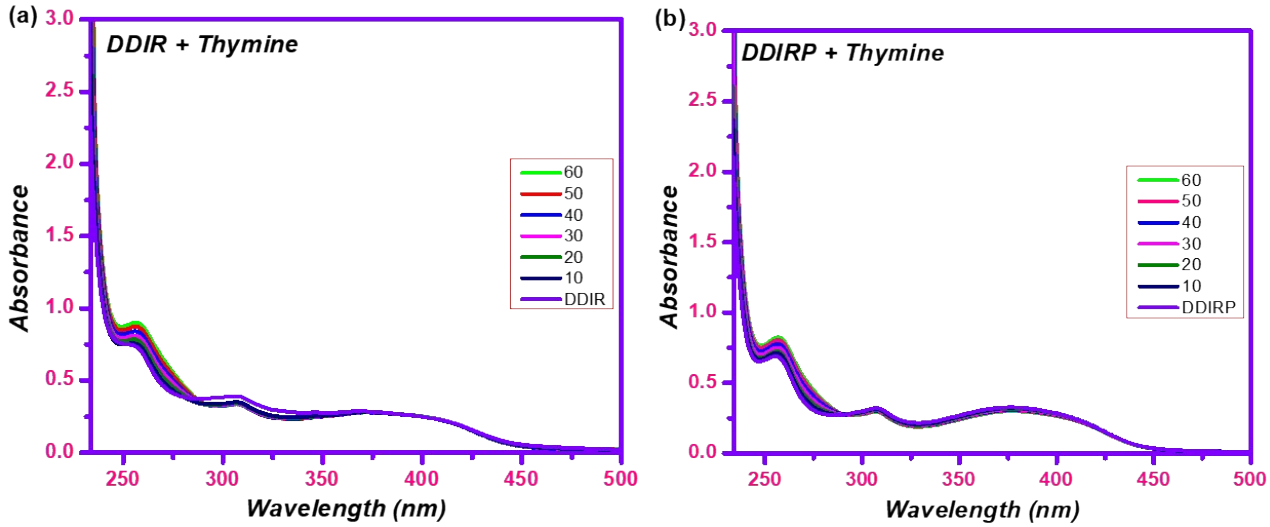

Fig. S25: Concentration-dependent binding study of DDIR (a) and DDIRP (b) complexes with 1 mM Thymine solution.

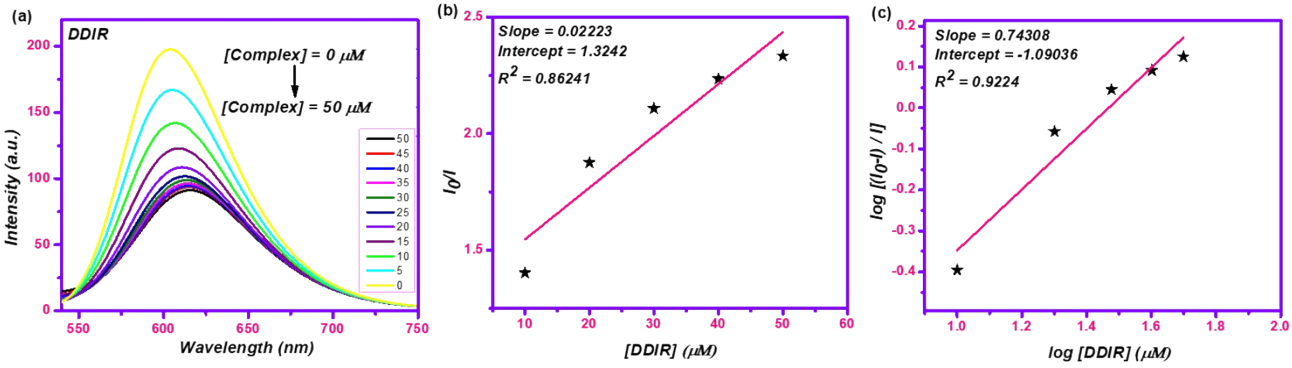

Fig. S26: (a) Interaction of complex DDIR with EtBr, (b) Stern-Volmer plot of I_0/I vs concentration of complex DDIR, (c) Scatchard plot of log [I_0-I/I] vs log [complex] for EtBr in presence of complex DDIR.

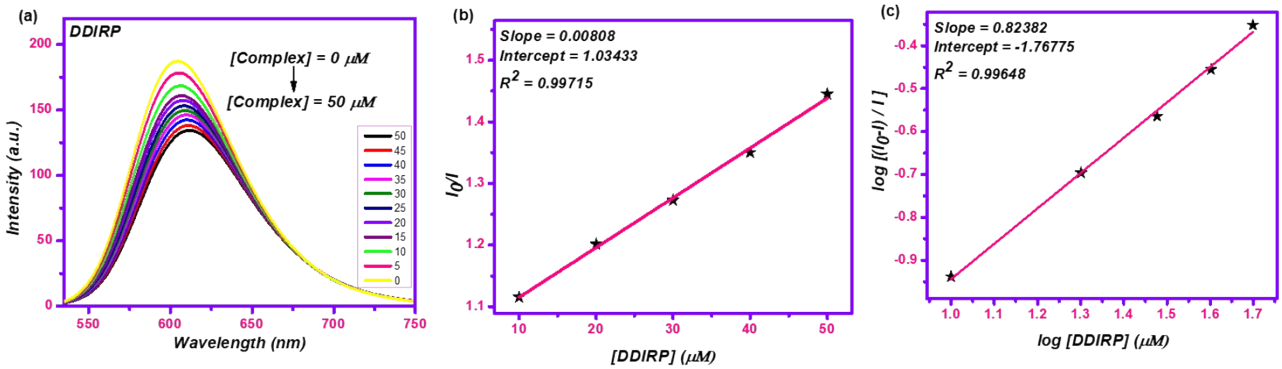

Fig. S27: (a) Interaction of complex DDIRP with EtBr, (b) Stern-Volmer plot of I_0/I vs concentration of complex DDIRP, (c) Scatchard plot of log $[I_0-I/I]$ vs log [complex] for EtBr in presence of complex DDIRP.

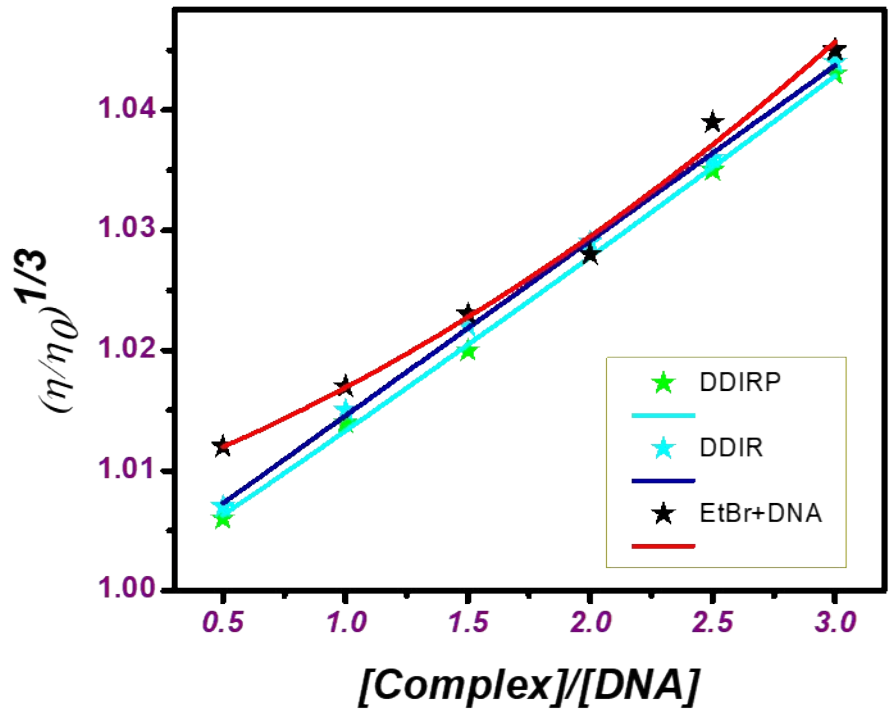

Fig. S28: Relative viscosity plot of ct-DNA with complexes DDIR and DDIRP to EtBr at 25 ^{0}C.

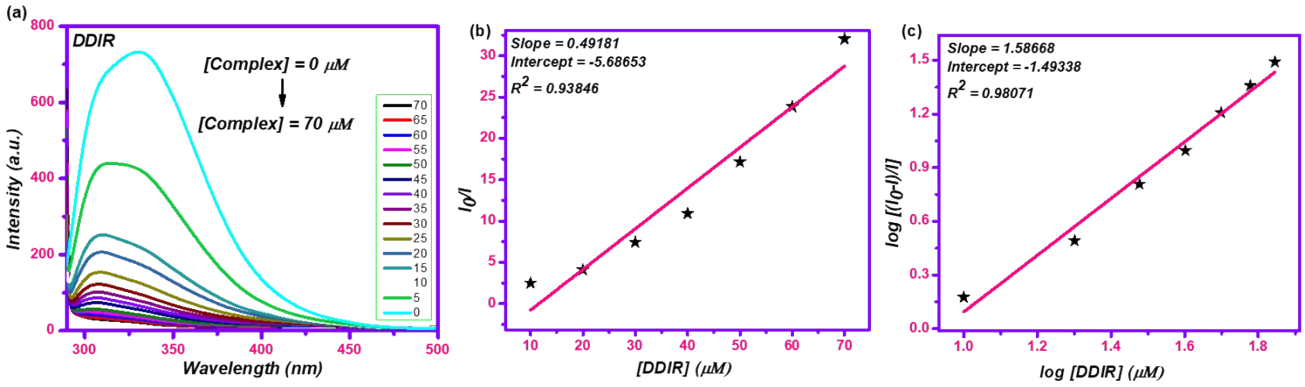

Fig. S29: (a) Interaction of complex DDIR with HSA, (b) Stern-Volmer plot of I_0/I vs concentration of complex DDIR, (c) Scatchard plot of log $[I_0-I/I]$ vs log [complex] for HSA in presence of complex DDIR.

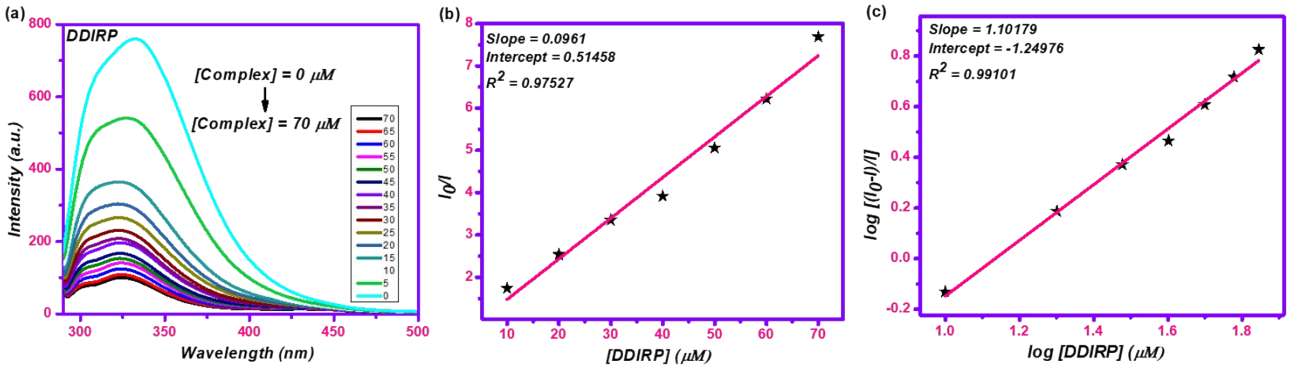

Fig. S30: (a) Interaction of complex DDIRP with HSA, (b) Stern-Volmer plot of I_0/I vs concentration of complex DDIRP, (c) Scatchard plot of log $[I_0-I/I]$ vs log [complex] for HSA in presence of complex DDIRP.

Table S1. Light and dark toxicity of all the synthesized complexes against HEK-293

Complex	IC_{50} (μM)[a]					
	HEK-293[c]					
	(in the absence of GSH)			(in the presence of GSH)		
	Dark	In light	PI[d]	Dark	In light	PI
DDIR	109.22±0.79	102.41±0.69	1.06	124.42±0.93	118.41±0.37	1.05
DDIRP	104.28±0.78	97.40±0.47	1.07	109.12±0.76	97.40±0.59	1.12
Cisplatin	48.52±0.42	47.13±0.88	1.01	66.46±0.62	65.23±0.46	1.01

[a] IC_{50}: 50% of cells experience cell death. [b]HEK-293 cell line. [c] immortalized human embryonic kidney cell lines. [d]PI: Phototoxicity index